Permittivity and Loss Characterization of SU-8 Films for mmW and Terahertz Applications

Nima Ghalichechian, *Senior Member, IEEE*, and Kubilay Sertel, *Senior Member, IEEE*

***Abstract*—The dielectric permittivity measurement of thick SU-8 film is presented for the entire frequency band of 1 GHz to 1 THz. SU-8 is a high-resolution UV-patternable photoresist that can be used for fabrication of high-aspect-ratio 3-D structures for millimeter-wave and terahertz devices. Here, we report the measured dielectric constant and loss tangent of SU-8 films using terahertz time-domain spectroscopy. A quadratic polynomial model is established for the accurate calculation of complex permittivity up to 1 THz. The loss tangent of fully cross-linked 430-μm-thick SU-8 film was measured to be 0.015, 0.027, and 0.055 at 1, 200, and 1000 GHz, respectively. Similarly, relative permittivity was found to be 3.24, 3.23, and 2.92. The fabrication process and level of cross-linking were demonstrated to have significant impact on the loss behavior of this material and the impact of cross-linking on dielectric permittivity is quantified across a wide frequency band. The characterization results reported in this letter are a platform for developing next-generation millimeter-wave and terahertz devices.**

***Index Terms*—Loss tangent, millimeter-wave (mmW), permittivity, SU-8, terahertz, time-domain spectroscopy.**

I. Introduction

AMONG available dielectric materials for millimeter-wave (mmW) and terahertz (THz) applications, SU-8 is particularly attractive due to its low loss and ability to form thick and high-resolution structures. SU-8 is a high-contrast epoxy-based UV-patternable negative photoresist, commonly used in the fabrication of high-aspect-ratio thick (0.5–200 μm) microelectromechanical systems (MEMS) and devices [1]. Low molecular weight of SU-8 results in high solubility ($> 85\%$) of solid resin inside the polymer matrix. Together with low optical absorption (to UV light), these features enable the fabrication of thick UV-patternable layers with vertical side-walls using standard spin-coating techniques. Furthermore, since the polymer is epoxy-based, it exhibits excellent adhesion to inorganic substrates and high resistance to harsh chemicals that are typically used in microfabrication processes, such as electroplating. These unique attributes make SU-8 film suitable for wafer-level integration of wideband mmW antennas with RF front ends and digital baseband circuits for system-on-chip (SoC) applications.

Fabrication process development for ultra-thick (> 400 μm) SU-8 films as well as the understanding of the electrical properties of SU-8 play a vital role in realization of such highly integrated systems. Specifically, the characterization of the permittivity of this film is crucial for efficient design of the future mmW and THz devices. Previous literature on SU-8 permittivity reports a wide range of measured data using varying fabrication recipes for a narrow frequency band. As an example, the loss tangent ($\tan\delta$) of 500-μm-thick SU-8 film was measured at 1 THz by time-domain spectroscopy to be 6.3×10^{-6} by one group [2] and 1.4×10^{-1} by another [3]. Permittivity measurements at lower frequencies are more consistent from one study to another. Using a microstrip ring resonator, Dewdney *et al.* reported a dielectric constant of 3.2 at 4 GHz [4]. Collins *et al.* used an SU-8 filled waveguide and reported $\varepsilon_{\rm r} = 1.725 \pm 0.08$ and $\tan\delta = 0.02 \pm 0.001$ at 75–110 GHz [5]. Mbairi and Hesselbom used conductor-backed coplanar waveguide transmission lines with SU-8 as a dielectric medium that resulted in estimation of $\varepsilon_{\rm r} = 3.25$ and $\tan\delta = 0.027$ at 30 GHz [6]. In the latter approach, the effective permittivity is first extracted from S-parameter measurements. An analytical model or simulation is then used (with a few simplifying assumptions) to extract the relative permittivity $\varepsilon_{\rm r}$. However, since the transmission-line losses are dominated by radiation, conductor, and dielectric losses, precise determination of dielectric loss depends highly on the accuracy of the radiation and conductor loss estimations. The latter are often estimated using numerical simulations and could have large errors. Similar to coplanar waveguides, a microstrip line can also be used for these measurements. For instance, Ghannam *et al.* found $\varepsilon_{\rm r} = 2.85$ and $\tan\delta = 0.04$ at 15 GHz [7], while a manufacturer reported $\varepsilon_{\rm r} = 4.1$ (at 50% relative humidity) and $\tan\delta = 0.015$ at 1 GHz [8].

Unlike the aforementioned waveguide-based measurements, free-space techniques such as THz time-domain spectroscopy do not suffer from the inaccuracies listed above. The discrepancies in the reported values of permittivity and loss are also the result of the differences in the fabrication process for SU-8 in addition to the errors in the measurement approach and the data analysis. In our work, we have addressed these shortcomings and built a reliable database for SU-8 permittivity covering the range of 200 GHz–1 THz. Moreover, we demonstrate that our results can be extrapolated beyond the measured frequency range down to 1 GHz. This was further verified with measurements conducted at 1 GHz. In the following, we discuss sample preparation and fabrication, followed by details of the measurement setup and analytical model that was developed for accurate

Manuscript received October 03, 2014; accepted December 06, 2014. Date of publication December 11, 2014; date of current version March 02, 2015. This work was supported in part by the State of Ohio Third Frontier Program through the Wright Center for Sensor Systems and Engineering.

The authors are with the ElectroScience Laboratory, Department of Electrical and Computer Engineering, The Ohio State University, Columbus, OH 43212 USA (e-mail: ghalichechian.1@osu.edu; sertel.1@osu.edu).

Color versions of one or more of the figures in this letter are available online at http://ieeexplore.ieee.org.

Digital Object Identifier 10.1109/LAWP.2014.2380813

extraction of permittivity and loss tangent of thick SU-8 films. Subsequently, a discussion of the results and the analysis of loss behavior are presented.

II. Fabrication of Ultra-Thick SU-8 Films

Two sets of SU-8 samples were prepared for this study: partially cured (Sample I) and fully cured films (Sample II). SU-8 2100 photo-patternable epoxy solution from Microchem Corp. was used to prepare thick films on 100-mm-diameter fused silica wafers. The substrates were first cleaned with acetone, methanol, isopropanol, and deionized water and dehydrated on a hotplate at 200° C for 20 min. Several SU-8 films with thickness of 330–450 μm were spin-coated and soft-cured at 95°C for 45 min. Wafers were then rested for 5 h in a vacuum desiccator to relax the film stress. This step was proven to eliminate approximately 90% of film cracks that would have normally appeared on the surface after final processing steps. Wafers were then exposed using an i-line UV lithography system with a dose of 900 mJ/Cm^2 followed by curing at 95°C for 15 min. Sample II was further cured at 150°C for 10 min to achieve full cross-linking or near-100% polymerization. SU-8 films were then removed from the silica substrate upon rapid cool down inside an acetone solution. Released samples, approximately 20 mm in diameter, were rinsed and dried with a nitrogen (N_2) gun.

III. THz-TDS Measurement Setup

A commercial THz-TDS system (TPS Spectra 3000 from TeraView, Ltd.) was used to measure the amplitude and phase of the transmitted electric field through SU-8 samples. Calibration and sample measurements were performed in N_2 dry environment to remove the impact of water vapor and O_2 absorption lines. Measurements were performed at 60 GHz–3 THz, however, due to low signal-to-noise ratio, only the 200 GHz–1 THz data were used in our analysis. The frequency resolution of our setup was 3.59 GHz (0.12 cm^{-1}) with each point measured and averaged 300 times to remove any random errors originating from laser amplitude fluctuations.

For initial estimation of dielectric permittivity as well as validation of our approach, we used empirical values measured using a material impedance analyzer (Agilent E4991A with 16453A dielectric test fixture) [9]. As an example, for a fully cured SU-8 film, we measured $\varepsilon'_{\rm r} = 2.85$ and $\tan\delta = 0.016$ at 1 GHz. The film thickness for each sample was measured using a micrometer instrument having standard deviation of measurement error $\delta_{\rm e} = 0.4$ μm. The measured thicknesses, together with real and imaginary components of the permittivity, were used as initial input to the transmission coefficient model described in the following.

IV. Analytical Model for Dielectric Permittivity of Thick SU-8 Films

Terahertz TDS is a coherent free-space measurement technique in which both the amplitude and the phase of the transmitted (or reflected) electric field of a pulsed wave are measured [10], [11]. This enables the measurement of the real and imaginary components of the refractive index $\tilde{n}(f)$, as a function of frequency, without requiring potentially inaccurate estimations using Kramers–Kronig relations [12]. Here, we use transmission-mode THz-TDS, where the time-domain response of the electric field is measured twice with and without the SU-8 sample. The ratio of the Fourier-transformed electric field for the sample, $E_{\rm Sample}(f)$, to the air reference, $E_{\rm Ref}(f)$, provides the complex transmission coefficient $T(f)$. The signal passes through the air ($n = 1$) on the two sides of the sample, then enters and exits the medium under measurement with backward and forward reflections, i.e., the Fabry–Pérot effect. As outlined in [13], the complex transmission coefficient can thus be written as

$$T(f) = \frac{E_{\rm Sample}(f)}{E_{\rm Ref}(f)} = \frac{\frac{4\tilde{n}(f)}{(\tilde{n}(f)+1)^2}\exp\left(-j\frac{2\pi f(\tilde{n}(f)-1)}{c}d\right)}{1-\frac{(\tilde{n}(f)-1)^2}{(\tilde{n}(f)+1)^2}\exp\left(-j\frac{4\pi f\tilde{n}(f)}{c}d\right)} \tag{1}$$

where d is the thickness of the sample and c is the speed of light. Equation (1) assumes a plane wave entering an isotropic and homogeneous medium at a normal incident. Furthermore, the sample is assumed to be flat with a uniform thickness. In (1), the relative permittivity is related to the refractive index via $\tilde{\varepsilon}_{\rm r}(f) = \tilde{n}(f)^2$. Alternatively, the relative permittivity is defined as $\tilde{\varepsilon}_{\rm r}(f) = \varepsilon'_{\rm r}(f) - j\varepsilon''_{\rm r}(f)$. In this letter, we focus on the accurate measurement of the real and imaginary components of the permittivity, as well as the loss tangent defined as $\tan\delta(f) = \varepsilon''_{\rm r}(f)/\varepsilon'_{\rm r}(f)$.

In order to accurately determine $\varepsilon'_{\rm r}(f)$ and $\varepsilon''_{\rm r}(f)$, we constructed a transmission coefficient model using (1) through iterative nonlinear least-squares method to fit to the measured data. In this approach, the SU-8 film thickness (d), $\varepsilon'_{\rm r}(f)$, and $\varepsilon''_{\rm r}(f)$ are all assumed unknown. For the real component of the permittivity, a second-order frequency-dependent binomial with constant and leading terms in the form of $\varepsilon'_{\rm r}(f) = \alpha_1 + \alpha_2 f^2$ is used, where f is the frequency in THz. Similarly, we use a second-order polynomial in the form of $\varepsilon''_{\rm r}(f) = \alpha_3 + \alpha_4 f + \alpha_5 f^2$ for the imaginary part. This model results in six independent variables that need to be estimated through the iterative method.

We must note that one of the drawbacks of this approach is the sensitivity of the final result on the initial valuations. In particular, care must be taken to estimate the initial values for the film thickness, as well as the relative permittivity. These initial values can be simply estimated using a quick measurement described in Section III. For the data fitting, we use the residual sum of squares, viz.

$$\sum_{i=1}^{n}\left(T_i^{\rm model} - T_i^{\rm measured}\right)^2 \tag{2}$$

as a cost function. In (2), $T_i^{\rm model}$ and $T_i^{\rm measured}$ are the calculated and measured transmission coefficients of the $|T(f)|$ ith point, respectively.

V. Experimental Results

As outlined in Sections III and IV, the transmission coefficients measured using THz-TDS were analyzed and compared to the model for two sets of samples. Fig. 1 shows the transmission coefficient amplitude $|T(f)|$ for experimental and fitted results. The top and bottom figures, respectively, show the transmission results for partially cross-linked and fully cross-linked

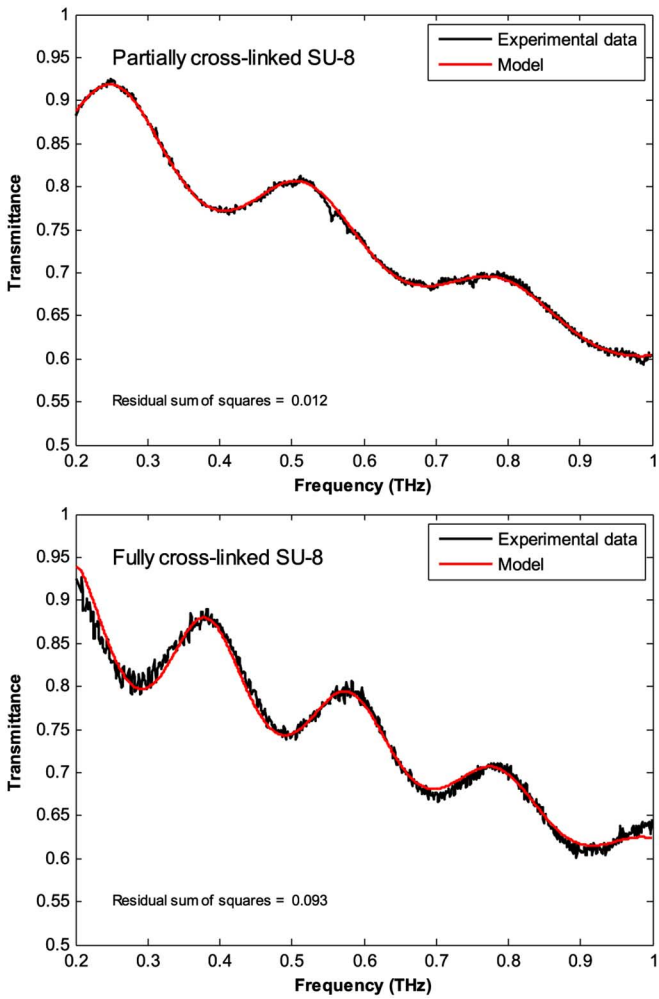

Fig. 1. Experimental and computed transmission coefficient, $|T(f)|$, for *(top)* partially and *(bottom)* fully cross-linked SU-8 samples showing excellent agreement between the two. Residual sum of squares, from (2), is also shown.

samples. Based on (1), the number of peaks, (N_{p}), in Fig. 1 is correlated to the thickness of sample and the real part of permittivity $(\varepsilon_{\mathrm{r}}')$ of the medium, by

$$\Delta f \approx \frac{c}{2d\sqrt{\varepsilon_{\mathrm{r}}'}} N_{\mathrm{p}} \tag{3}$$

where Δf is the distance between two adjacent peaks on the transmission plot. It is worth noting that (3) can also be used for rough estimation of $\varepsilon_{\mathrm{r}}'$. On the other hand, the loss tangent of the medium impacts the level of transmission amplitude.

Fig. 2 shows the real part of permittivity as a function frequency. From 200 GHz to 1 THz, $\varepsilon_{\mathrm{r}}'$ declines from 3.2 to 2.9 and 2.9 to 2.7, respectively, for fully and partially cross-linked films. Fig 2 also depicts $\varepsilon_{\mathrm{r}}''$ or the imaginary part of the permittivity on the same plot.

The loss tangents for the two samples are shown in Fig 3. For a fully cross-linked film, $\tan\delta$ is measured to be 0.027 and 0.055 at 200 GHz and 1 THz, respectively. However, the measured values for partially cross-linked film were on average 66% higher and found to be 0.045 and 0.075, respectively. Table I summarizes the results for the estimated thickness as well as the extracted α_n coefficients for real and imaginary permittivity of the SU-8 samples. In the formula, the units

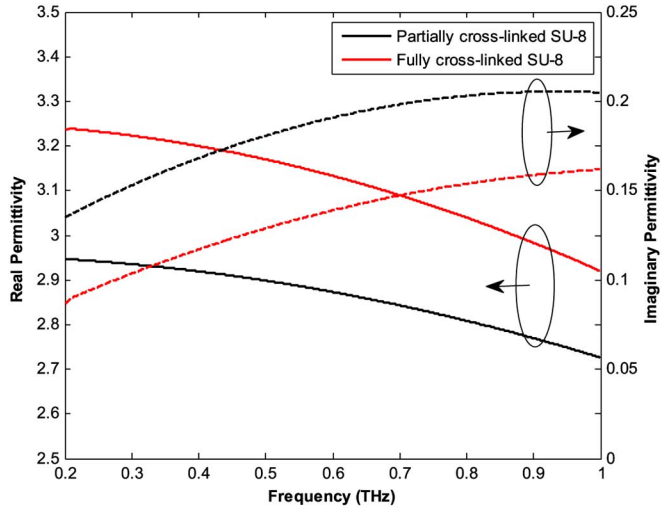

Fig. 2. Measured real (left axis) and imaginary (right axis) permittivity as a function of frequency for two types of SU-8.

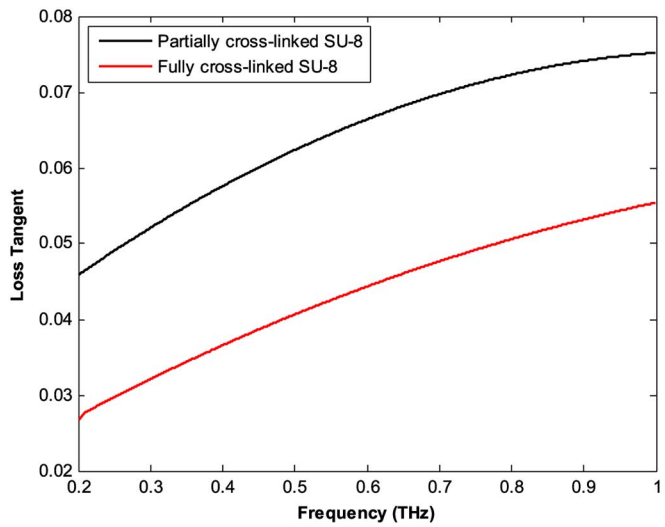

Fig. 3. Measured loss for SU-8 showing the frequency response of the dielectric and significantly larger losses for partially cured sample.

TABLE I
MEASURED THICKNESS AND COEFFICIENTS FOR SU-8 COMPLEX PERMITTIVITY FUNCTIONS FOR 200 GHz–1 THz

Symbol	PARTIALLY CROSS-LINKED	FULLY CROSS-LINKED
d, μm	332.4	433.8
α_1	2.95	3.25
α_2	–0.22	–0.33
α_3	–0.09	–0.05
α_4	–0.24	–0.20
α_5	0.13	0.09

$\epsilon_r'(f) = \alpha_1 + \alpha_2 f^2$ & $\epsilon_r''(f) = \alpha_3 + \alpha_4 f + \alpha_5 f^2$.

of the frequency variable f are in THz. In the following, we discuss the SU-8 permittivity behavior at different frequencies and its dependence on the fabrication process.

VI. Discussion

There are several factors impacting the permittivity and loss tangent of SU-8 at various frequencies. Among them are the level of cross-linking/polymerization, impurities, solvent, and moisture content. We attempted to minimize the impact of moisture content by performing measurements in a N_2-purged chamber and the solvent content by preparing samples with identical soft bake steps (as discussed in Section II). This controlled experiment enables isolating the impact of polymerization on the permittivity and material losses. The measurement results show that partially cross-linked samples exhibit on average 66% larger loss tangent (at 200 GHz) compared to fully cross-linked SU-8. Therefore, baking the SU-8 film at 150°C or higher is recommended to reduce dielectric loss for mmW and THz devices. Furthermore, both samples show large dispersion resulting in significantly higher losses at higher frequencies, most likely due to dipolar (rotational) polarization. As an example, for a fully cross-linked sample, losses approximately double from 0.027 (200 GHz) to 0.055 (1 THz). Moreover, the real permittivity is fairly constant for two samples and reduces by only 8%–10% from 200 GHz to 1 THz.

Our model can also be expanded to lower frequencies. For instance, using the values in Table I, loss tangent for a fully cross-linked film is extracted to be 0.015 at 1 GHz, which is in line with material impedance analyzer measurement ($\tan\delta = 0.016$) and the reported value by the manufacturer ($\tan\delta = 0.015$) [8]. Similarly, losses for the entire mmW band can be extracted. As an example, using our model given in Table I, at 60 GHz the expected $\tan\delta = 0.019$ compared to 0.02 at 75 GHz reported by [5]. As seen, the permittivity depends highly on the cure temperature during sample fabrication.

There are multiple sources of systematic and random uncertainty in THz-TDS measurements. Among them are amplitude variation of THz signal, sample roughness, thickness uniformity, alignment, approximations of transfer functions, and errors in data analysis [14]. In our measurements, we have attempted to address random errors by repeating and averaging measurements. To address some of the systematic errors, we did not use a simple extraction or smoothing/filtering methods that it is often used in literature where (1) is approximated and Fabry–Pérot effects are neglected. Instead, we used iterative nonlinear least-squares fit for transmission coefficient and extracted the permittivity values using (1). Additionally, the scattering effect of THz wave from the detection path, although small, results in smaller transmission and consequently larger approximation for the loss tangent. Therefore, we expect the real losses to be slightly lower than the reported values.

Compared to other dielectric materials, SU-8 shows loss tangent that is smaller than PMMA, polyester, and polyamide (typically $\tan\delta > 0.06$). On the other hand, SU-8 shows larger losses than benzocyclobutene (BCB), HDPE, polypropylene, and Teflon ($\tan\delta < 0.02$). However, none of the low-loss materials mentioned above can achieve thick, high-resolution, and high-aspect-ratio features. For instance, BCB film has $\varepsilon_r = 2.4$ and $\tan\delta = 9 \times 10^{-3}$ at 1 THz [15], but can only achieve maximum thickness of 30 μm, which is 15 times smaller than SU-8.

VII. Conclusion

A systematic characterization of dielectric permittivity of thick SU-8 films at 1 GHz–1 THz was reported. Time domain spectroscopy was used to measure the transmission of the THz wave for fully and partially cured SU-8 samples. An analytical model for complex transmission coefficient, including the Fabry–Pérot effects, was considered for accurate extraction of SU-8 permittivity. The measurement setup and analysis technique were verified for other materials such as Teflon and can be used for a range of dielectric films in addition to SU-8. Moreover, while the measurement was performed at 200 GHz–1 THz, our technique results in accurate estimation of dielectric properties down to 1 GHz. The ability to fabricate thick, high-resolution structures with vertical sidewalls makes SU-8 attractive for integration of antennas and other devices on wafer. Compared to other techniques, such as silicon deep reactive ion etching (DRIE), SU-8 provides a spin-on additive process with the ability to define features lithographically. Understanding the dielectric properties of SU-8 plays an important role on efficient design of future mmW and THz devices, such as, on-chip ultrawideband antennas and frequency selective surfaces.

References

[1] H. Lorenz *et al.*, "High-aspect-ratio, ultrathick, negative-tone near-UV photoresist and its applications for MEMS," *Sensors Actuators A, Phys.*, vol. 64, pp. 33–39, Jan. 1, 1998.

[2] S. Arscott *et al.*, "Terahertz time-domain spectroscopy of films fabricated from SU-8," *Electron. Lett.*, vol. 35, pp. 243–244, 1999.

[3] S. Lucyszyn, "Comment on Terahertz time-domain spectroscopy of films fabricated from SU-8," *Electron. Lett.*, vol. 37, p. 1267, 2001.

[4] J. M. Dewdney and J. Wang, "Characterization the microwave properties of SU-8 based on microstrip ring resonator," in *Proc. 10th Annu. IEEE WAMICON*, 2009, pp. 1–5.

[5] C. E. Collins *et al.*, "Millimeter-wave measurements of the complex dielectric constant of an advanced thick film UV photoresist," *J. Electron. Mater.*, vol. 27, pp. 40–42, 1998.

[6] F. D. Mbairi and H. Hesselbom, "High frequency design and characterization of SU-8 based conductor backed coplanar waveguide transmission lines," in *Proc. Int. Symp. Adv. Packag. Mater.*, 2005, pp. 243–248.

[7] A. Ghannam, C. Viallon, D. Bourrier, and T. Parra, "Dielectric microwave characterization of the SU-8 thick resin used in an above IC process," in *Proc. EuMC*, 2009, pp. 1041–1044.

[8] Microchem Corp., Westborough, MA, USA, "Microchem Corp.," 2014 [Online]. Available: http://www.microchem.com

[9] N. Ghalichechian, J. P. Doane, W. Hong, K. Sertel, and J. L. Volakis, "Characterization of SU-8 using terahertz time-domain spectroscopy," in *Proc. AP-S/USNC-URSI Symp.*, 2013, p. 18.

[10] M. Naftaly and R. E. Miles, "Terahertz time-domain spectroscopy for material characterization," *Proc. IEEE*, vol. 95, no. 8, pp. 1658–1665, Aug. 2007.

[11] C. A. Schmuttenmaer, "Exploring dynamics in the far-infrared with terahertz spectroscopy," *Chem. Rev.*, vol. 104, pp. 1759–1779, 2004.

[12] P. H. Bolivar *et al.*, "Measurement of the dielectric constant and loss tangent of high dielectric-constant materials at terahertz frequencies," *IEEE Trans. Microw. Theory Tech.*, vol. 51, no. 4, pp. 1062–1066, Apr. 2003.

[13] L. Duvillaret, F. Garet, and J.-. Coutaz, "A reliable method for extraction of material parameters in terahertz time-domain spectroscopy," *IEEE J. Sel. Topics Quantum Electron.*, vol. 2, no. 3, pp. 739–746, Sep. 1996.

[14] W. Withayachumnankul, B. M. Fischer, H. Lin, and D. Abbott, "Uncertainty in terahertz time-domain spectroscopy measurement," *J. Opt. Soc. Amer. B*, vol. 25, pp. 1059–1072, 2008.

[15] E. Perret, N. Zerounian, S. David, and F. Aniel, "Complex permittivity characterization of benzocyclobutene for terahertz applications," *Microelectron. Eng.*, vol. 85, pp. 2276–2281, 2008.